

Supporting Information

***In Situ* Dual-Modification Strategy for O₃-NaNi_{1/3}Fe_{1/3}Mn_{1/3}O₂ towards High-Performance Sodium-Ion Batteries**

Ningyun Hong^a, Jianwei Li^c, Shihong Guo^a, Huawei Han^a, Haoji Wang^b, Xinyu Hu^b, Jiangnan Huang^b, Baichao Zhang^b, Fang Hua^a, Bai Song^f, Nesrin Bugday^c, Sedat Yasar^c, Serdar Altin^d, Wentao Deng^{b,*}, Guoqiang Zou^b, Hongshuai Hou^b, Zhen Long^{a,*}, Xiaobo Ji^{b,*}

^a Tianjin Key Laboratory of Functional Crystal Materials, Institute of Functional Crystal, College of Material Science and Engineering, Tianjin University of Technology, Tianjin, China

^b State Key Laboratory of Powder Metallurgy, College of Chemistry and Chemical Engineering, Central South University, Changsha, China

^c Department of Chemistry, Inonu University, Malatya, Turkey

^d Department of Physics, Inonu University, Malatya, Turkey

^e Key Laboratory of Comprehensive and Highly Efficient Utilization of Salt Lake Resources, Qinghai Institute of Salt Lakes, Chinese Academy of Sciences (CAS), Xining, China

^f Dongying Cospowers Technology Limited Company, China

Supplementary Note:

The Na⁺ chemical diffusion coefficients for GITT results can be calculated by the Weppner and Huggins equation:

$$D_{\text{GITT}} = \frac{4}{\pi\tau} \left(\frac{m_B V_M}{M_B S} \right)^2 \left(\frac{\Delta E_s}{\Delta E_\tau} \right)^2 \quad (\tau \ll L^2/D) \quad (1)$$

Where m_B , M_B , S , and V_M are the molecular weight, mass and molar volume of the cathode electrode, respectively. S and L represent the surface area and average radius of the active material particles. ΔE_s and ΔE_τ are steady-state voltage and the total change of the cell voltage during the current pulse process.

For CV results, the apparent Na⁺ diffusion coefficients D_{Na^+} can be calculated based on the Randles-Sevcik equation:

$$I_p = 2.69 \times 10^5 n^{3/2} A D_{\text{Na}^+}^{1/2} \nu^{1/2} \Delta C_0 \quad (2)$$

Where I_p is the peak current, n denotes the electron transfer number of the reaction, A represents the electrode area of the cathode, ν represents the scan rate, and ΔC_0 is the concentration of Na⁺ in the lattice.

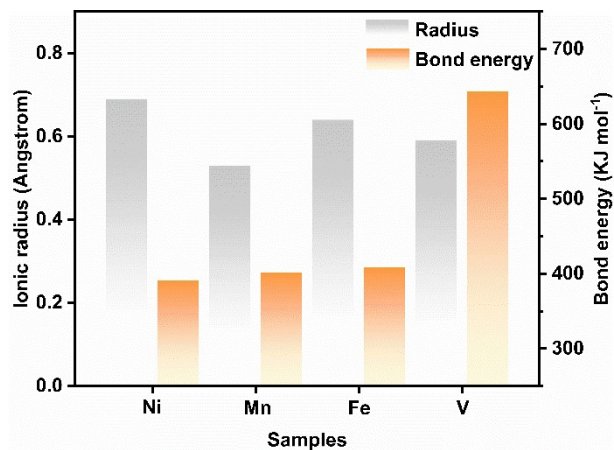


Fig. S1. The comparison of ionic radius and bonding energy with different elements.

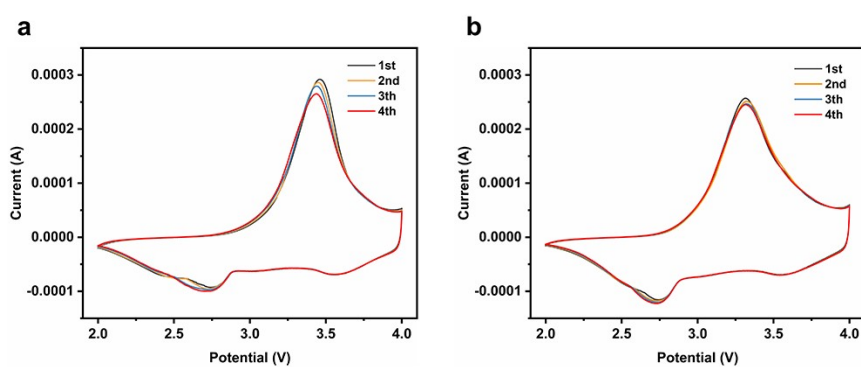


Fig. S2. (a-b) The initial four CV curves at a scanning rate of 0.1 mV s^{-1} for NFM and NFMV-1.

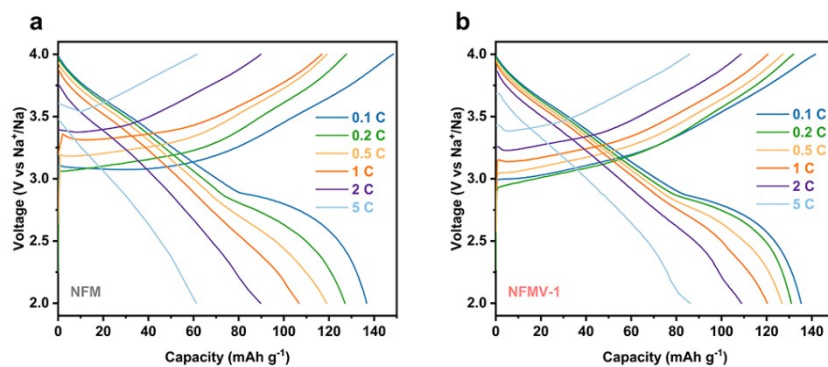


Fig. S3. (a-b) GCD curves at different current rate for NFM and NFMV-1.

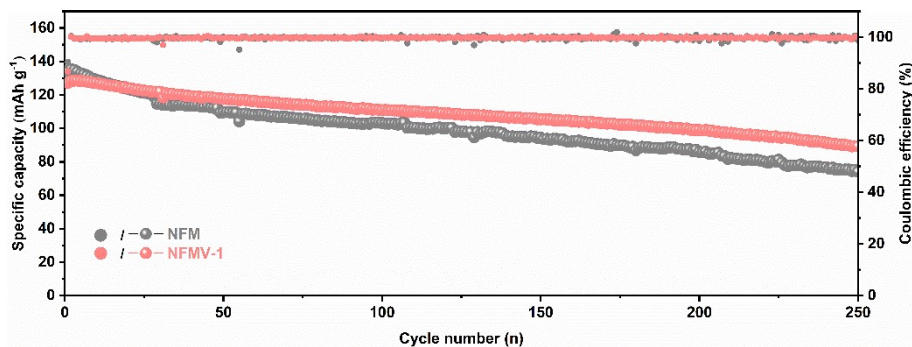


Fig. S4. Long-term cycling performance of NFM and NFMV-1 at 1 C at the voltage from 2.0-4.2 V

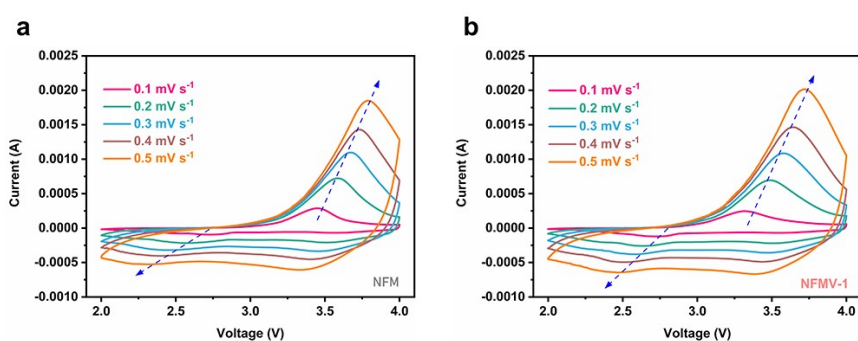


Fig. S5. (a-b) GCD curves at different scan rate for NFM and NFMV-1.

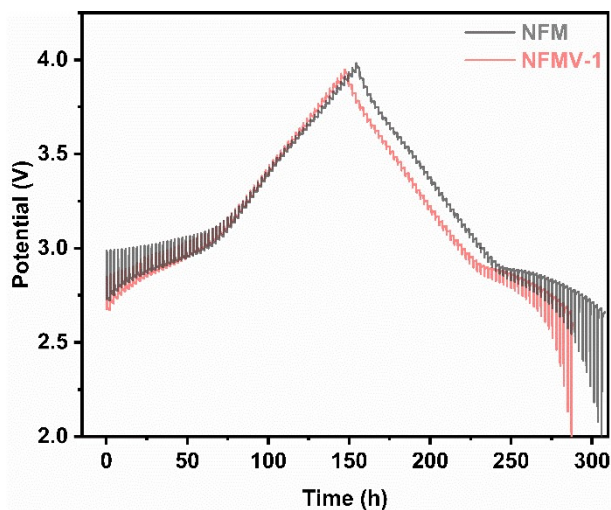


Fig. S6. Transient voltage-time profile obtained from GITT test for the obtained Samples.

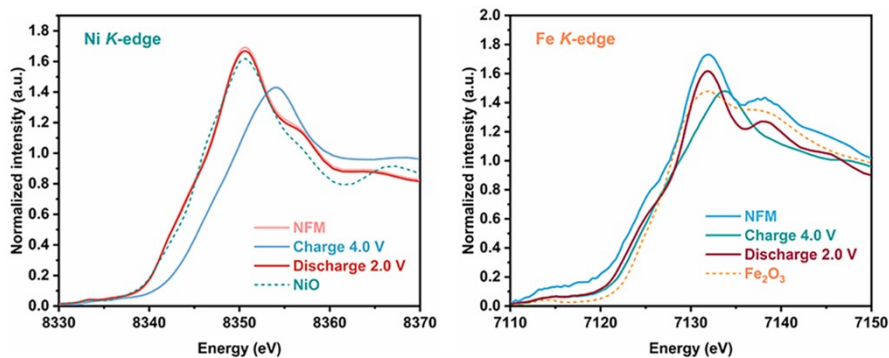


Fig. S7. Ni/Fe K-edge of NFM under different charging state.

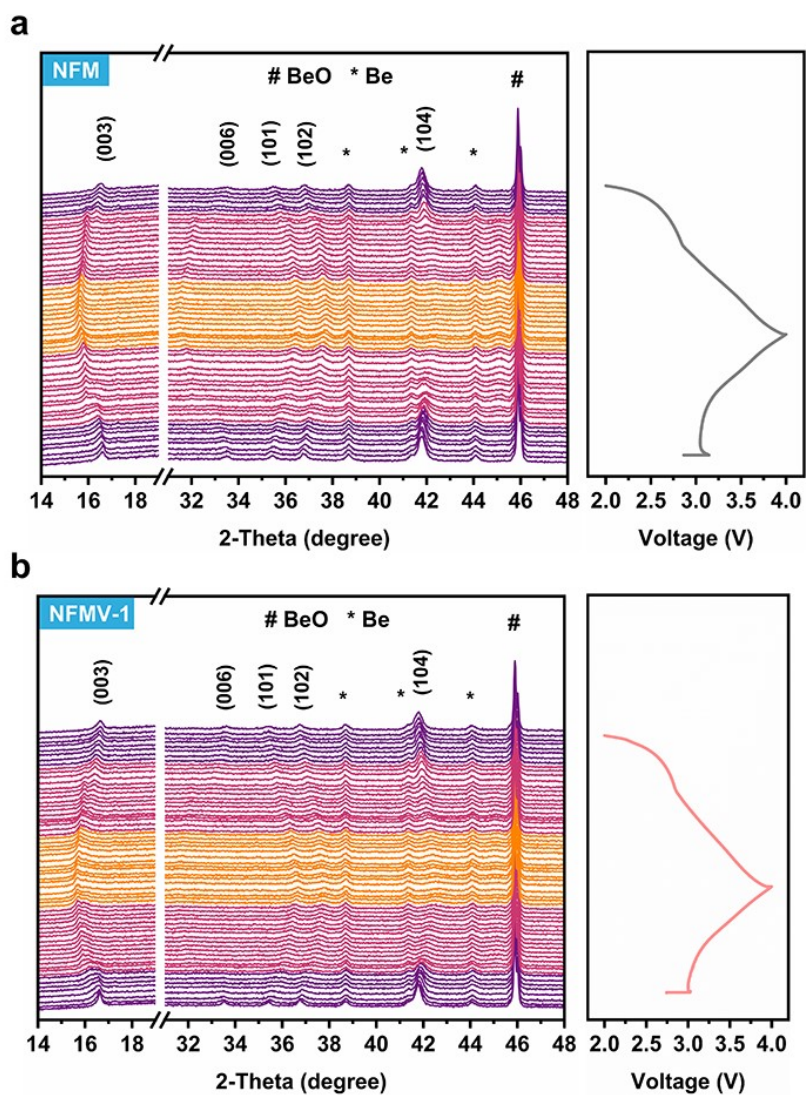


Fig. S8. In situ XRD patterns collected during the first charge/discharge of NFM and NFMV-1 over a voltage range of 2.0-4.0 V.

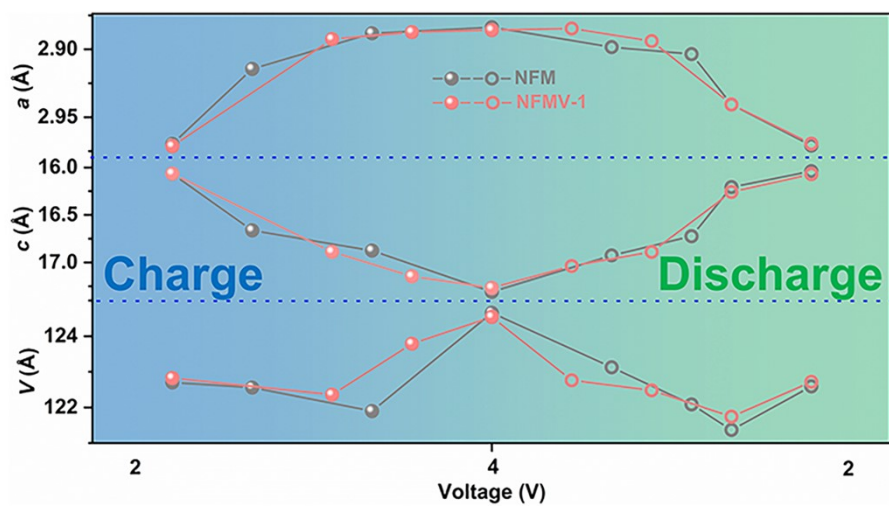


Fig. S9. The detailed change of lattice parameters of selected electrodes during the cycling process.

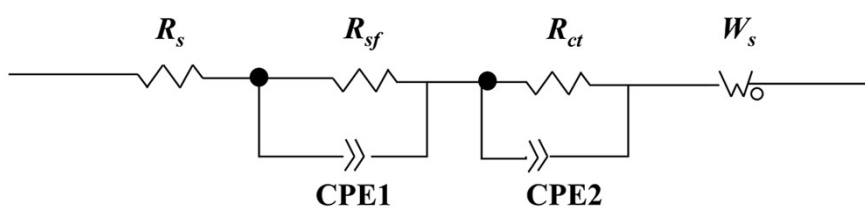


Fig. S10. equivalent circuit of EIS.

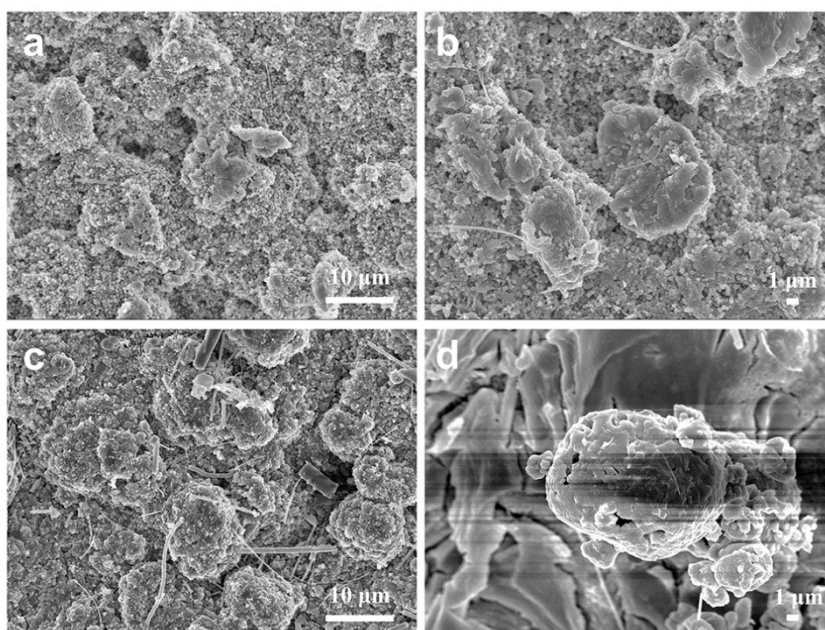


Fig. S11. SEM image of the of cycled cathodes for (a-b) NFM, (c-d)NFMV-1.

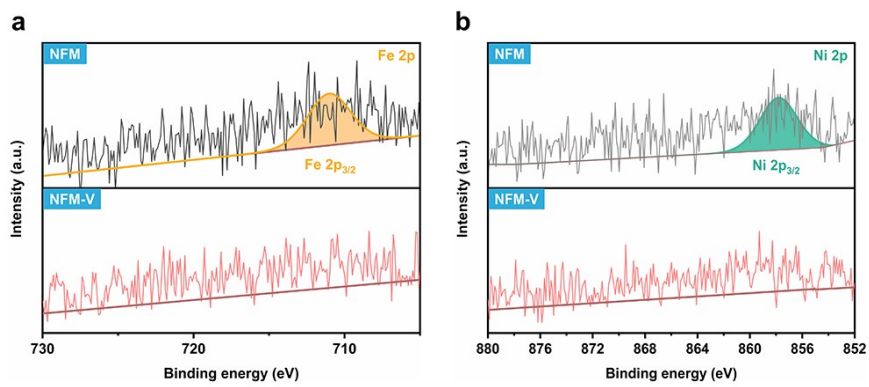


Fig. S12. XPS results of cycled cathodes for selected elements.

Table S1. ICP-OES results of all the samples.

Theoretical chemical formula	Measured atomic ratio				
	Na	Ni	Mn	Fe	V
$\text{NaNi}_{0.333}\text{Mn}_{0.333}\text{Fe}_{0.333}\text{O}_2$	1.003	0.337	0.335	0.333	0
$\text{NaNi}_{0.331}\text{Mn}_{0.331}\text{Fe}_{0.331}\text{V}_{0.005}\text{O}_2$	1.001	0.333	0.332	0.331	0.0048
$\text{NaNi}_{0.330}\text{Mn}_{0.330}\text{Fe}_{0.330}\text{V}_{0.010}\text{O}_2$	1.006	0.328	0.330	0.329	0.0106
$\text{NaNi}_{0.328}\text{Mn}_{0.328}\text{Fe}_{0.328}\text{V}_{0.015}\text{O}_2$	0.997	0.325	0.329	0.323	0.0140

Table S2. Crystallographic data and refinement parameters of all the samples.

Samples	NFM	NFMV-0.5	NFMV-1	NFMV-1.5
a, b [Å]	2.9788	2.9775	2.9742	2.9722
c [Å]	16.0304	16.0375	16.0518	16.0578
α, β [°]	90	90	90	90
γ [°]	120	120	120	120
V [Å ³]	123.189	123.134	122.972	122.85
R_p [%]	1.75	4.35	1.31	1.51
R_{wp} [%]	2.47	5.58	1.86	2.05

Table S3. Atomic distances, slab thickness and d-spacing of the Na layer for NFM and NFMV-1 from XRD refinement.

Samples	NFM	NFMV-1
TM-O [Å]	2.089	2.076
Na-O [Å]	2.272	2.284
TMO ₂ [Å]	2.372	2.336
Na-spacing [Å]	2.970	3.014
Interlayer [Å]	5.342	5.350

Table S4. The calculated diffusion coefficients by GITT test for (a) NFM, (b) NFMV-1.

Samples	Charge	Discharge
	D_{Na^+} [10^{-11} cm ² s ⁻¹]	D_{Na^+} [10^{-11} cm ² s ⁻¹]
NFM	6.80	3.95
NFMV-1	12.32	5.94

Table S5. EIS test results for (a) NFM, (b) NFMV after different cycled.

Samples	R_s (Ω)	R_{sf} (Ω)	R_{ct} (Ω)
NFM-uncycled	5.4	0	257.0
NFMV-uncycled	5.4	0	153.2
NFM-after 2 cycled	5.4	0	274.1
NFMV-after 2 cycled	5.6	0	164.8
NFM-after 500 cycled	7.2	469.7	734.2
NFMV-after 500 cycled	7.0	218.0	587.4

Table S6. Comparison of cycling performances of V-NFM with other modified NFM cathodes.

Cathode	Voltage window (V)	Cycling stability	Ref.
NVO-NFM	2.0-4.0 V	75.8%, 500, 2 C	This work
		96.4%, 150, 0.5 C	
NFM	2.0-4.0 V	50.7%, 500, 2 C	This work
		74.2%, 150, 0.5 C	
Zn-NFM	2.0-4.0 V	86.53%, 200, 1C	1
F-NFM	2.0-4.0 V	90%, 70, 1C	2
ZrO ₂ -NFM	1.5-4.0 V	86%, 100, 1 C	3
MoF-NFM	2.0-4.0 V	91.97%, 100, 1C	4
NTP-NFM	1.5-4.2 V	77.5%, 100, 1C	5
Sn-NFM	2.0-4.1 V	75%, 150, 0.5C	6

Table S7. Crystallographic and Rietveld refinement data of the NFM cathode.

Atom	Wyckoff position	x	y	z	Occ.
Na	3b	0	0	0	1
Ni	3a	0	0	0.5	0.333
Mn	3a	0	0	0	0.333
Fe	3a	0	0	0	0.333
O	6c	0	0	0.25933(14)	1

Table S8. Crystallographic and Rietveld refinement data of the NFMV-1 cathode.

Atom	Wyckoff position	x	y	z	Occ.
Na	3b	0	0	0	1
Ni	3a	0	0	0.5	0.330
Mn	3a	0	0	0	0.330
Fe	3a	0	0	0	0.330
V	3a	0	0	0	0.010
O	6c	0	0	0.26055(10)	1

Table S9. EXAFS fitting results for Fourier transformed $k^3 \times (k)$ Ni K-edges structural parameters of samples.

Samples	Atom	X-Y pair	CN	R (Å)	$\sigma^2 / (10^{-2} \text{Å}^2)$	ΔE_0 (eV)	R-factor
NFM	Ni-O	Ni-O	6	2.06929	0.779	-5.558	0.006
	Ni-TM	Ni-TM	6	2.95681	0.720		
NFMV-1	Ni-O	Ni-O	6	2.09134	0.983	-2.752	0.014
	Ni-TM	Ni-TM	6	2.99016	0.719		

CN: coordination number; R: bond length; σ^2 : Debye-Waller factor (disorder); ΔE_0 : energy parameter.

Table S10 Transition metal ion dissolution results of cycled batteries.

Sample	Concentration (ug/L)		
	Ni	Fe	Mn
NFM	276.34	650.53	16.93
NFMV-1	154.35	443.78	15.89

Reference

1. W. Qin, Y. Liu, J. Liu, Z. Yang and Q. Liu, *Electrochimica Acta*, 2022, **418**.
2. Q. Zhang, Y. Huang, Y. Liu, S. Sun, K. Wang, Y. Li, X. Li, J. Han and Y. Huang, *Science China Materials*, 2017, **60**, 629-636.
3. Y. Yu, D. Ning, Q. Li, A. Franz, L. Zheng, N. Zhang, G. Ren, G. Schumacher and X. Liu, *Energy Storage Materials*, 2021, **38**, 130-140.
4. W. Li, Q. Chen, D. Zhang, C. Fang, S. Nian, W. Wang, C. Xu and C. Chang, *Materials Today Communications*, 2022, **32**.
5. S. Zhao, Q. Shi, R. Qi, X. Zou, J. Wang, W. Feng, Y. Liu, X. Lu, J. Zhang, X. Yang and Y. Zhao, *Electrochimica Acta*, 2023, **441**.
6. T. Song, L. Chen, D. Gastol, B. Dong, J. F. Marco, F. Berry, P. Slater, D. Reed and E. Kendrick, *Chem Mater*, 2022, **34**, 4153-4165.